



**HAL**  
open science

# Investigation Properties of Pervious and Water-Retaining Recycled Concrete to Mitigate Urban Heat Island Phenomena

Bechara Haddad, Hamzé Karaky, Mohamed Boutouil, Bertrand Boudart,  
Nassim Sebaibi

► **To cite this version:**

Bechara Haddad, Hamzé Karaky, Mohamed Boutouil, Bertrand Boudart, Nassim Sebaibi. Investigation Properties of Pervious and Water-Retaining Recycled Concrete to Mitigate Urban Heat Island Phenomena. *Sustainability*, 2023, 15 (6), 10.3390/su15065384 . hal-04035103

**HAL Id: hal-04035103**

**<https://hal.science/hal-04035103>**

Submitted on 17 Mar 2023

**HAL** is a multi-disciplinary open access archive for the deposit and dissemination of scientific research documents, whether they are published or not. The documents may come from teaching and research institutions in France or abroad, or from public or private research centers.

L'archive ouverte pluridisciplinaire **HAL**, est destinée au dépôt et à la diffusion de documents scientifiques de niveau recherche, publiés ou non, émanant des établissements d'enseignement et de recherche français ou étrangers, des laboratoires publics ou privés.

## Article

# Investigation Properties of Pervious and Water-Retaining Recycled Concrete to Mitigate Urban Heat Island Phenomena

Bechara Haddad <sup>1,\*</sup>, Hamzé Karaky <sup>1</sup>, Mohamed Boutouil <sup>1</sup>, Bertrand Boudart <sup>2</sup> and Nassim Sebaibi <sup>1</sup>

<sup>1</sup> Builders Lab, Builders Ecole d'Ingénieurs, ComUE Normandie Université, 1 Rue Pierre et Marie Curie, 14610 Epron, France

<sup>2</sup> Normandie Université, UNICAEN, ENSICAEN, CNRS, GREYC, 14000 Caen, France

\* Correspondence: bechara.haddad@builders-ingenieurs.fr; Tel.: +33-2-31-46-23-00

**Abstract:** The urban heat island (UHI) effect poses significant challenges to urban environmental quality and public health. Over the decades, research efforts have been made to develop various UHI mitigation strategies, including pavement materials, such as, water-retentive pavement, reflective pavement, and pervious concrete. This paper focuses on the improvement of the hygric and water retention properties of pervious concrete to mitigate UHI phenomena. The hydric and hygroscopic tests were carried out under dry and wet conditions on four different pervious concretes, where natural aggregates were replaced with recycled aggregates at different mass percentages. The results show a significant improvement in these properties by increasing the amount of recycled aggregates incorporated in the mixtures. The mixes made from recycled aggregates alone showed an absorption that reached 75 L more than the control in one cubic meter under wet condition. With an upwelling capacity of up to 30 kg of retained water in a square meter under dry condition, these improvements in water performance represent this permeable concrete as a water retention pavement solution for UHI mitigation. Regarding the mechanical properties, a decrease of 50% in compressive strength was noted only when 100% of the recycled aggregate was incorporated, remaining at 20 MPa for other mixtures.



**Citation:** Haddad, B.; Karaky, H.; Boutouil, M.; Boudart, B.; Sebaibi, N. Investigation Properties of Pervious and Water-Retaining Recycled Concrete to Mitigate Urban Heat Island Phenomena. *Sustainability* **2023**, *15*, 5384. <https://doi.org/10.3390/su15065384>

Academic Editors: José Ignacio Alvarez and Marinella Giunta

Received: 16 January 2023

Revised: 27 February 2023

Accepted: 14 March 2023

Published: 17 March 2023



**Copyright:** © 2023 by the authors. Licensee MDPI, Basel, Switzerland. This article is an open access article distributed under the terms and conditions of the Creative Commons Attribution (CC BY) license (<https://creativecommons.org/licenses/by/4.0/>).

**Keywords:** pervious concrete; hydric properties; urban heat island

## 1. Introduction

The phenomenon of urban heat islands (UHIs) arises from the interplay between the built environment and anthropogenic activities, resulting in elevated temperatures in urban regions vis à vis suburban and rural areas [1–3]. This temperature differential is primarily driven by variations in the heat balance between constructed surfaces, such as roads and buildings, and natural surfaces, such as vegetation and soil, which exhibit divergent thermal properties and thermal inertia. Specifically, the low thermal inertia and light coloration of natural surfaces enable efficient reflection, thus promoting cooling via evapotranspiration and reducing sensible heat. Conversely, constructed surfaces possess high thermal inertia and dark pigmentation, which facilitate the accumulation and retention of solar radiation, thereby exacerbating sensible heat and warming the urban atmosphere [4–6].

Pavements, which constitute a considerable fraction (20–40%) of urban surfaces, are significant contributors to the formation of UHIs [7]. Consequently, a wealth of research has been directed towards mitigating the impact of UHIs through cooling pavement surfaces. One promising approach involves irrigating surfaces with recycled wastewater, an intervention already implemented in cities such as Tokyo and Osaka, where irrigation systems deploy recycled water to spray surfaces through water supply pipes [8,9]. Another promising avenue is the development of cool pavements, which can enhance solar reflectance, evaporation, and/or reduce sensible heat in the urban environment via innovative pore structure designs, high-absorbing fillers, or reflective surfaces [10–12]. These pavements

can be classified as reflective, evaporative, or water-trapping, and represent a promising tool in UHI mitigation [13–15].

The current research endeavors to explore the feasibility of augmenting the hygric capacity of pervious concrete through the incorporation of recycled aggregates, thereby enhancing the water retention capability of the pavement system and extending its evaporative cooling effect to mitigate UHIs. The focus is to optimize the use of pervious concrete in conjunction with other UHI mitigation strategies, such as surface watering, to develop a pervious concrete pavement that is both cool and retains water. To achieve this, it is essential to carefully balance the hydric/hygric properties of the pavement system with its drainage capabilities, by selecting the optimal proportion of recycled aggregates [16–25]. Notably, the mitigation of UHIs is a complex challenge that warrants a multifaceted approach that leverages a diversity of solutions and techniques.

The rapid pace of urbanization worldwide has led to surging demand for raw materials, with France alone consuming an estimated 400 million tons of aggregates annually, or six tons per capita, according to the French Union of Aggregates Producers [26]. This expansion of urban areas has also led to significant volumes of construction and demolition waste, resulting in pressing waste management and pollution issues. Addressing these challenges requires the urgent utilization of recycled aggregates and other substitutes that not only reduce pollution levels but also conserve natural resources, as highlighted in numerous reports [27–32].

In the current study, recycled aggregate (RA) provided from building demolition was utilized as a replacement for natural aggregate in the production of cool water-retaining pervious concrete, owing to its high moisture absorption capacity. The physical properties of the raw recycled aggregate were analyzed and compared to those of natural aggregate, with a focus on its hygroscopic and hydric characteristics. This innovative approach of this study was to assess the potential of using recycled aggregate to enhance the properties of pervious concrete and achieve a more efficient cool water-retaining pavement system.

To effectively utilize recycled aggregate as a replacement for natural aggregate in the production of cool water-retaining pervious concrete, a meticulously designed formulation and granulometry were employed. A specific compaction protocol was also implemented to ensure that the functional mechanical properties of the concrete were maintained while maximizing its hygric and hygroscopic properties. This approach aimed to enhance the water retention properties of the pervious concrete and mitigate the urban heat island effect.

## 2. Materials and Methods

### 2.1. Materials

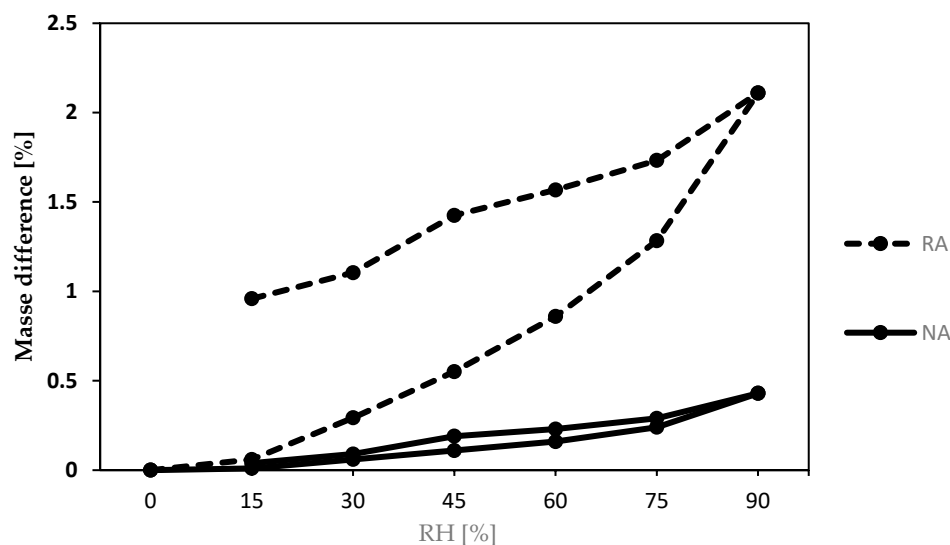
The production of pervious concrete involves the use of fundamental materials: water, cement, and coarse aggregates. This study utilized ordinary Portland cement (OPC) CEM I 52.5R, characterized by a specific surface area of  $4525 \text{ cm}^2/\text{g}$  and a specific gravity of  $3.14 \text{ g/cm}^3$ . The cement exhibited a 28-day compressive strength of 67 MPa. The chemical, physical, and mechanical properties of CEM I 52.5R cement are summarized in Table 1.

In this study, the production of pervious concrete involved the use of two types of coarse aggregate: recycled coarse aggregate (RA) and natural aggregate (NA). The recycled aggregates come from the demolition of buildings and the origin of the natural aggregates is alluvial gravel. RA was obtained by crushing and sieving raw recycled aggregates to obtain particles in the size range of 2 to 6.8 mm, which is the same as that of NA. No plasticizers or additional treatments were applied to RA in order to reduce production costs. The aggregate impact value (AIV) and aggregate crushing value (ACV) of RA were 1.5% and 14%, respectively, while those of NA were 5% and 23%. The results of the AIV and ACV tests indicate that RA has lower resistance to impact and crushing compared to NA. This is likely due to the presence of attached mortar on RA, which tends to detach under impact and abrasion loading, leading to reduced resilience.

**Table 1.** Chemical and physical properties of cement CEM I 52.5 R.

Chemical Analysis (%)				Physical and Mechanical Characteristics	
Loss on ignition	1.4	Na <sub>2</sub> O	0.11	Initial setting time (min)	215
SiO <sub>2</sub>	20	P <sub>2</sub> O <sub>5</sub>	0.2	Specify gravity (g/cm <sup>3</sup> )	3.14
Al <sub>2</sub> O <sub>3</sub>	5.4	S <sup>-</sup>	0.04	Specific surface Blaine (cm <sup>2</sup> /g)	4525
Fe <sub>2</sub> O <sub>3</sub>	2.7	Cl <sup>-</sup>	0.03	Compressive strength (MPa)	
TiO <sub>2</sub> /MnO	-	Insoluble	0.2	1j	30
CaO	63	Na <sub>2</sub> O eq/Active	0.75	2j	44
MgO	1.9	C <sub>3</sub> A	-	7j	57
SO <sub>3</sub>	3.7	C <sub>3</sub> A + 0.27C <sub>3</sub> S	-	28j	67

In addition, since the aim of this work is to investigate the effect of RA on the hygric properties of pervious concrete, sorption/desorption tests were conducted on both natural and recycled aggregates. The results, shown in Figure 1, indicate that recycled aggregates (RA) exhibit a mass absorption of 2.2% at a relative humidity of 90%, while natural aggregates (NA) only show a mass absorption of 0.43%. Additionally, Table 2 presents additional physical and hygric characteristics of both aggregates. It should also be noted that alluvial quartz sand with a specific gravity of 2620 kg/m<sup>3</sup>, a fineness modulus of 2.81, a grain size of 0/2 mm, and an absorption coefficient of 0.50% was used in all the mixes.

**Figure 1.** Sorption/desorption curves for recycled and natural aggregates.**Table 2.** Physical and chemical properties of recycled and natural aggregates.

	Standard	RA	NA
Absolute specific gravity (kg/m <sup>3</sup> )	NF EN 1097-6 [33]	2270	2600
Water absorption coefficient (%)	NF EN 1097-6 [33]	6.6	1.02
Fineness modulus (%)	NF EN 933-1 [34]	0.33	0.32
Micro-Deval test (%)	NF EN 1097-1 [35]	22	11

## 2.2. Mix Composition and Preparation

To achieve an optimal mixture of pervious concrete, a comprehensive approach is needed to balance mechanical strength and hygric properties. In this study, an optimal mixture was developed by balancing these factors.

### 2.2.1. Cement Content

The cement content used in this study was  $363 \text{ kg/m}^3$ , falling within the range of 270 to  $415 \text{ kg/m}^3$  reported in previous research [23,36,37].

### 2.2.2. Aggregate Density

The literature shows that the density of the aggregate component in pervious concrete mixtures can vary significantly. Optimal ranges have been reported as ranging from 1190 to  $1800 \text{ kg/m}^3$  [36,37]. In addition, the grain size distribution of aggregates is a critical factor that influence porosity and mechanical resistance [38,39]. In consequence, we conducted multiple trials to identify an optimal grain size distribution (2–6.8 mm) and aggregate dosage ( $1574 \text{ kg/m}^3$ ) that would provide a satisfactory balance of mechanical and hydric properties, with and without recycled aggregates (RA). The G/C ratio in this study was 4.3, falling within the recommended range of 4 to 4.5, according to the relevant literature [24,37].

### 2.2.3. Sand Dosage

Previous research [38,40,41] suggests that a uniform dosage of  $110 \text{ kg/m}^3$  of sand is typically used. This dosage falls within the range of  $100 \text{ kg/m}^3$  and is below the maximum allowable limit of  $175 \text{ kg/m}^3$ , as determined by relevant research [40].

### 2.2.4. Water Content

On the other hand, it is critical to carefully control the water content in pervious concrete mixtures, as variations in water levels can significantly impact the resulting properties of the concrete, specially hydric and mechanical properties, as stated in the literature [39,42–45]. The appropriate range for the water-to-cement ratio (W/C) in the presence of admixtures is between 0.27 and 0.34, while the range increases from 0.34 to 0.40 in the absence of admixtures [23,46,47].

In this study, no admixtures were used, and a water dosage of  $129 \text{ kg/m}^3$ , resulting in a W/C ratio of 0.35, was selected. Given the high water absorption capacity of the recycled aggregates (RA) used in this study (which is six times higher than that of natural aggregates, as seen in Table 2), an additional mass of water equivalent to 90% of the RA's absorption capacity was added to the mix.

### 2.2.5. Final Mix Design

Table 3 presents a summary of the optimal values and reported ranges of key parameters relevant to the mix design of pervious concrete. The preparation of the pervious concrete mixtures involved the use of four different formulations, as indicated in Table 4. Mixtures B, C, and D were formulated with 20%, 60%, and 100% recycled aggregate, respectively, while Mix A served as the control mixture with no recycled aggregate. The casting process involved the use of cubic specimens, which were subjected to vibration, and along with precise masses, achieved a pressure of 15 kPa [48].

## 2.3. Test Methods

### 2.3.1. Compressive Test

In the current test, three cubic specimens with dimensions of  $15 \times 15 \times 15 \text{ cm}$  from each formulation were used for testing. The specimens were cured for 28 days before being subjected to compression tests at a loading rate of  $0.06 \text{ MPa.s}^{-1}$ , in accordance with the NF EN 12390 standard [49].

### 2.3.2. Splitting Test

The measurement is performed on three  $15 \times 15 \times 15 \text{ cm}$  cubes with an imposed loading rate of  $0.05 \text{ MPa.s}^{-1}$ , according to NF EN 1338 [50].

**Table 3.** Optimal values and reported ranges of key parameters for pervious concrete mix design.

Parameter	Optimal Value Determined in This Study	Range Reported in Literature
Cement content	363 kg/m <sup>3</sup>	270–415 kg/m <sup>3</sup> [23,36,37]
Aggregate density and size	1574 kg/m <sup>3</sup> (2–6.8 mm)	1190–1600 kg/m <sup>3</sup> [36]; 1300–1800 kg/m <sup>3</sup> [37]; 1190–1480 kg/m <sup>3</sup> [23]
Sand dosage	110 kg/m <sup>3</sup>	100–175 kg/m <sup>3</sup> [40]
Water dosage	129 kg/m <sup>3</sup>	129 kg/m <sup>3</sup> [37,39,42–45].
Water-to-cement ratio (W/C)	0.35	0.27–0.34 in the presence of admixtures [23,46,47] 0.34–0.40 in the absence of admixtures [23,46,47]
Guideline for G/C	4.3	4–4.5 [23,37]

**Table 4.** Composition of different mixes proposed.

Samples	Cement (kg/m <sup>3</sup> )	Water (kg/m <sup>3</sup> )	NA (kg/m <sup>3</sup> )	RA (kg/m <sup>3</sup> )	Sand (kg/m <sup>3</sup> )
A (control with natural aggregate)	363	129	1574	0	110
B20%	363	129	1259	314	110
C60%	363	129	629	944	110
D100%	363	129	0	1574	110

### 2.3.3. Porosity

The method described in this statement is based on the Archimedean growth principle, as supported by different references [39,51,52]. According to the NF ISO 5017 standard [53], the specimens were first saturated with water under vacuum in a desiccator. Three cubic specimens with dimensions of 15 × 15 × 15 cm from each formulation were used for testing. The porosity accessible to water was then calculated by considering the masses of the specimens in both water and air, using the following formula:

$$P_a = \left( \frac{M_{\text{air}} - M_{\text{dry}}}{M_{\text{air}} - M_{\text{water}}} \right) \times 100 \quad (1)$$

where

$P_a$  represents the open porosity [%];

$M_{\text{air}}$  represents the mass of the specimen after saturation in water [kg];

$M_{\text{water}}$  represents the mass of the specimen while submerged in water [kg];

$M_{\text{dry}}$  represents the mass of the dry sample [kg].

### 2.3.4. Permeability

The permeability of a material is a measure of its ability to allow the passage of a fluid, such as water, under the influence of a pressure gradient. The coefficient of permeability, denoted by  $K$ , is used to express this property, and is calculated using Darcy's law [54]. Two methods can be used to measure the permeability of a material: the constant head method and the falling head method [23–25]. The constant head method involves evaluating the permeability of a material using water heads of 100 mm, 200 mm, and 300 mm, and is typically used for materials with permeability coefficients greater than 10<sup>-2</sup> mm/s. The falling head method involves recording the permeability of a material with an initial water level of 140 mm, 240 mm, and 340 mm and a final height of 50 mm, and is suitable for

materials with permeability coefficients of less than 1 mm/s. The water permeability test device used for both methods is shown in Figure 2.

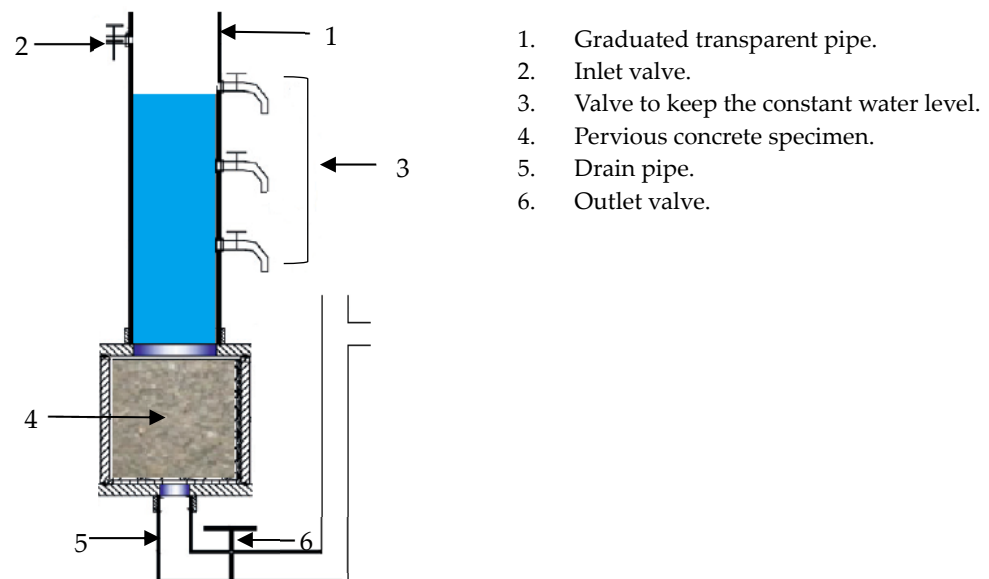


**Figure 2.** Measurement device of permeability coefficient for pervious concrete.

Three cubic specimens with dimensions of 15 × 15 × 15 cm from each formulation were used for testing. The permeability coefficient is determined using the following formulas at falling, and constant head respectively:

$$K = \left( \frac{A_{\text{tube}} - L}{A - t} \right) \times \ln \left( \frac{h_1}{h_2} \right) \quad (2)$$

$$K = \left( \frac{L}{h} \right) \times \frac{Q}{A(\Delta T)} \quad (3)$$

where

K represents the permeability coefficient (mm.s<sup>-1</sup>);

L represents the sample length (mm);

h represents the head of water (mm);

t represents the duration of water falling (seconds);

Q represents the volume of collected water (m<sup>3</sup>);

ΔT represents the duration of water collection (seconds);

A represents the cross-sectional area of specimen (mm<sup>2</sup>).

### 2.3.5. Water-Retaining and Absorption Coefficient

This test is conducted to evaluate the water-retaining capacity of pavement, as referenced in studies [55,56]. The pavement is first immersed in water at a surrounding temperature between 15–25 degrees Celsius for a duration of 24 h (see Figure 3). It is then removed from the water and the mass is monitored at intervals of 30 min for a total of 1 h and 30 min. Three cubic specimens with dimensions of 15 × 15 × 15 cm from each formulation were used for testing. The water capacity (W<sub>c</sub>) of the pavement is then calculated in kilograms per cubic meter (kg/m<sup>3</sup>) using the following formula:

$$W_c = \frac{W_{\text{wet}} - W_{\text{dry}}}{V} \quad (4)$$

where



$W_{\text{wet}}$  represents the mass of the specimen removed from water at different times (kg);  
 $W_{\text{dry}}$  represents the dry mass of the specimen (kg);  
 $V$  represents the volume of the specimen ( $\text{m}^3$ ).

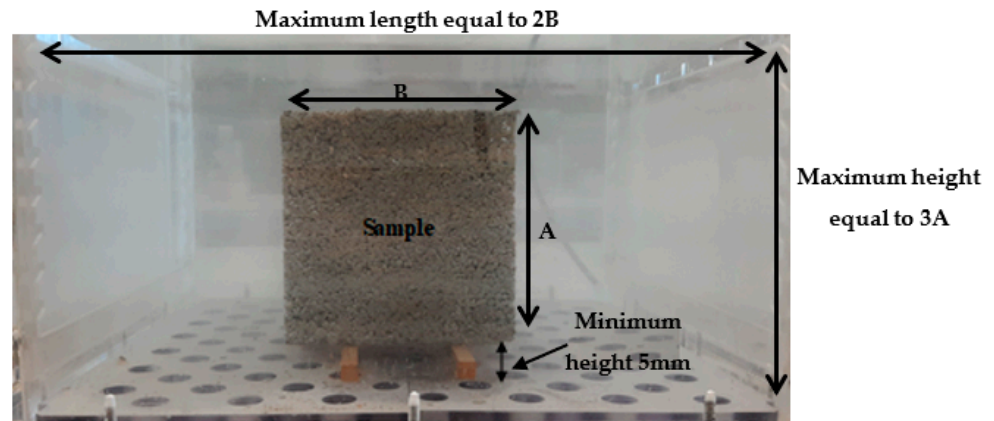


**Figure 3.** Schematic photograph of an apparatus for producing a wet state.

Additionally, the absorption coefficient is determined in accordance with the NF P 18-555 standard, which is the ratio of the increase in the mass of the sample after immersion in water for 24 h. The water absorption coefficient ( $A_b$ ) is defined by the following relation:

$$A_b = \frac{W_{\text{wet}} - W_{\text{dry}}}{W_{\text{dry}}} \quad (5)$$

### 2.3.6. Water Absorption Percentage and Capillarity Coefficient

This test is designed to evaluate the ability of the pervious concrete to retain water. This is to determine the suction height of the water. To do this, a dry pavement is placed in water, with 5 mm of the bottom surface submerged. The amount of water retained is then determined by monitoring the mass for a duration of 24 h minutes for each 10 min. This method is based on the protocol described in studies [55,56]. Three cubic specimens with dimensions of  $15 \times 15 \times 15$  cm from each formulation were used for testing. The water absorption value as a function of suction height (Sh) is then calculated in percent using the following formula:

$$Sh = \frac{W_h - W_{\text{dry}}}{W_{\text{wet}} - W_{\text{dry}}} \quad (6)$$

where

$W_h$  represents the mass of the sample in contact with water at different times (kg);  
 $W_{\text{wet}}$  represents the mass of the sample removed from water after saturation (kg);  
 $W_{\text{dry}}$  represents the dry mass of the samples (kg).

In addition, according to the NF EN 13057 standard, the capillarity absorption is determined by tracking the weight of the material exposed to water along its bottom surface for various immersion times (5, 15, 30, 60, 120, 240, 1440, 2880 min).

$$A_w = \frac{W_h - W_{\text{dry}}}{A} \quad (7)$$

where

$W_h$  represents the mass of the sample immersed in water (kg);  
 $W_{\text{dry}}$  represents the dry mass of the samples (kg);  
 $A$  represents the surface of contact between the sample and the water ( $\text{m}^2$ ).



### 2.3.7. Sorption/Desorption Test

The present study utilized the ProUmid SPSx-1 $\mu$  sorption/desorption system to investigate the sorption isotherms of mixes and raw material in accordance with ISO 12571 [57]. Three cubic specimens with dimensions of 5  $\times$  5  $\times$  5 cm from each formulation were used for testing. This system features a precision balance for the accurate measurement of sample mass, as well as precise temperature and humidity control to enable the study of sorption kinetics. The samples were dried to a constant weight (with a weight variation of less than 0.1%) prior to exposure to relative humidities ranging from 10% to 90% in five increments and then decrements at a temperature of 23 °C, as previously reported in studies [58,59].

## 3. Results and Discussion

### 3.1. Compressive and Splitting Test

The results of mechanical compression tests, as depicted in Figure 4a, indicate that Mixes A and C60% exhibited an identical compressive strength of 18 MPa. Mix B20% demonstrated an increase of 12% in compressive strength, with a value of 20 MPa. In contrast, mix D100% displayed a compressive strength of 8.5 MPa, representing a decrease of 55% compared to the control Mix A. On the other hand, the result of the splitting test in Figure 4b indicates that Mixes A, B20%, and C60% exhibited an identical splitting strength always above 2.5 MPa. In contrast, mix D100% displayed a splitting strength of 1.17 MPa, representing a decrease of 56% compared to the control Mix A.

This decrease is consistent with other findings [60], that observed a similar percentage of decrease when the natural aggregate was fully replaced with recycled aggregate. These results were obtained after 28 days of curing. It should be noted that for this type of concrete, 98.5% of its ultimate mechanical resistance is typically reached after 7 days of pouring [61,62].

The decrease in mechanical compressive strength and splitting strength observed in the concrete mixes containing recycled aggregate can be attributed to the insufficient bonding between the cement paste and the recycled aggregates [16,63]. This poor bonding is likely caused by the presence of residue and granular particles on the surface of the recycled aggregate [64,65]. Microscopic examination of the samples revealed that the bond between the cement paste and recycled aggregate was weak in mix D100%, where these particles were particularly dense. These particles formed a zone of preferential microcracking. In contrast, the presence of these particles did not significantly affect the propagation of cracks in Mixes B and C. Microscopic images comparing the control, Mix A, with the recycled aggregate, Mix D100%, highlight this weak adhesion. Furthermore, Figure 5 highlights the presence of these particles in Mix D100%, as compared to the control Mix A. The figure illustrates the impact of these particles on the propagation of cracks in the mix containing recycled aggregate. The figure suggests that the dense accumulation of these particles in Mix D100% may contribute to the preferential formation of microcracks, which may be responsible for the lower mechanical compressive strength observed in this mix.

In addition, the recycled aggregates used in the study have a higher absorption coefficient (6.6%) compared to natural aggregates (1%), as shown in Table 2. This higher absorption coefficient requires a “correction” factor to be applied to the water content in the mix design. However, it is difficult to accurately control this factor, which can lead to variations in the water-to-cement ratio. These variations can disturb the distribution of water in the cement mix, resulting in either an increase in mechanical strength (as seen in Mix B20%) or a decrease (as seen in Mix D100%).

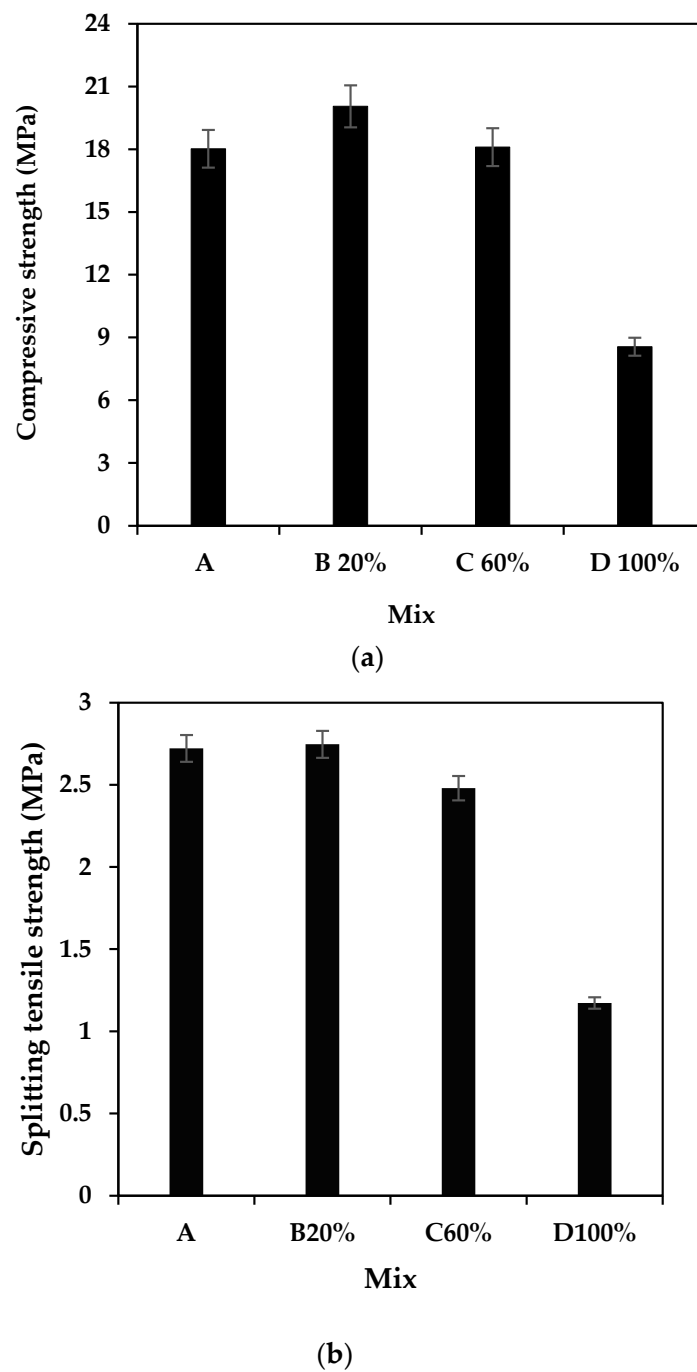


**Figure 4.** (a) Compressive strength of pavers  $15 \times 15 \times 15$  cm; (b) Splitting test of pavers  $15 \times 15 \times 15$  cm.

Moreover, recycled aggregates have lower physical properties than natural aggregates, as shown in Table 2. These properties include lower density and higher porosity, which results in concrete mixes that are more porous and less dense, and therefore, less resistant.

Despite the lower mechanical strength of mixes containing recycled aggregate, such mixes can still be used for certain applications. For example, drained pavers with a mechanical strength of at least 10 MPa can be used for parking precast pervious concrete products [63]. Paving stones with slightly lower mechanical strength can be used for walkways and pedestrian trails [66].

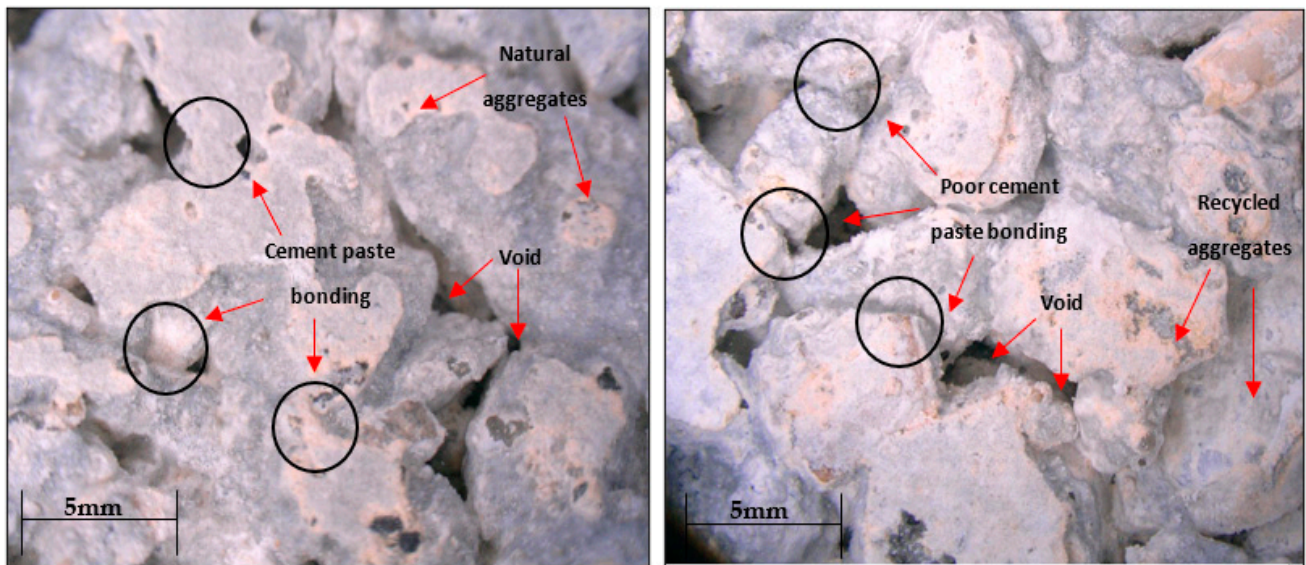


**Figure 5.** Comparison of aggregate-cement paste bonding for cubes specimens control A and D 100% mixtures.

### 3.2. Porosity

Figure 6 presents the porosity of water accessible to the different samples. It can be seen that the porosity increases slightly from Sample A to Sample C, with values of 24.7%, 25.2%, and 28.7%, respectively. However, Sample D exhibits significantly higher porosity at 36.9%. Previous research has indicated that the average porosity of a pervious pavement is typically within the range of 15–25%. Pavements with porosity values below 15% are not considered truly pervious [23,37,46,67].

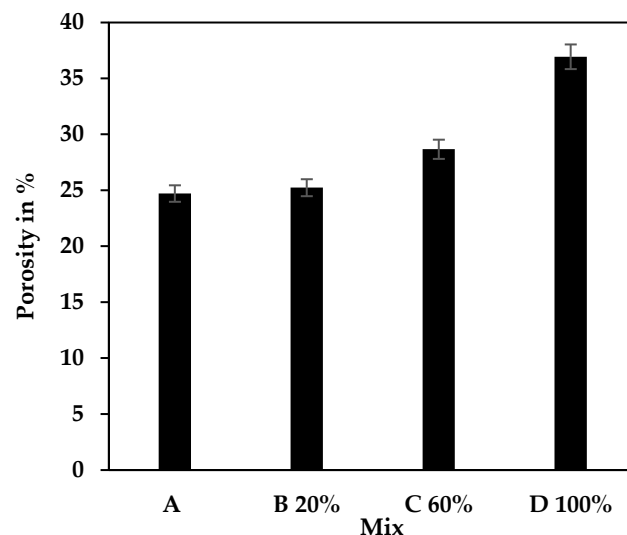


**Figure 6.** Porosity accessible to water for all mixtures.

The increase in porosity observed in the different mixes, which were composed of 20%, 60%, and 100% recycled aggregates, can be attributed to the presence of granular residue on the RA. This residue decreases the surface area of contact between the RA in the mixes, resulting in an increase in open porosity and a decrease in thermal inertia. The enhanced permeability and reduced thermal inertia of the surface that results from this increased porosity has several benefits. Permeable pavements with higher porosity have been shown to have lower temperatures at night and to cool more quickly than conventional pavements [68,69]. The incorporation of recycled aggregates (RA) in pavement mixtures

has been shown to be effective in creating a light pavement with low thermal inertia. This characteristic is beneficial in mitigating the urban heat island (UHI) effect during the nighttime period, as it allows the surface to cool more quickly. The presence of RA in the mixture also leads to an increase in hydric characteristics, which can further aid in mitigating the UHI effect during the daytime period [13,17,70]. These hydric characteristics, which will be discussed in greater detail in the interlocking section, may include increased moisture retention and evaporation, leading to a reduction in surface temperatures.

### 3.3. Permeability

Figures 7 and 8 illustrate the permeability coefficients determined through the application of the constant and falling head tests on all mixtures at various heads. The data depicted in these figures indicate that the permeability of the mixtures increases with the inclusion of higher percentages of recycled aggregates. This trend can be attributed to the increase in the porosity of the material, as demonstrated in Figure 9. The porosity of the mixtures increases with the incorporation of recycled aggregates, leading to an increase in the permeability of the material. It is important to note that the relationship between permeability and compressive strength in permeable concrete is inverse [71]. As the compressive strength of the material increases, the permeability decreases. This inverse relationship is due to the fact that an increase in compressive strength is typically achieved through the reduction in voids in the material, leading to a decrease in the overall porosity and permeability of the pervious concrete.

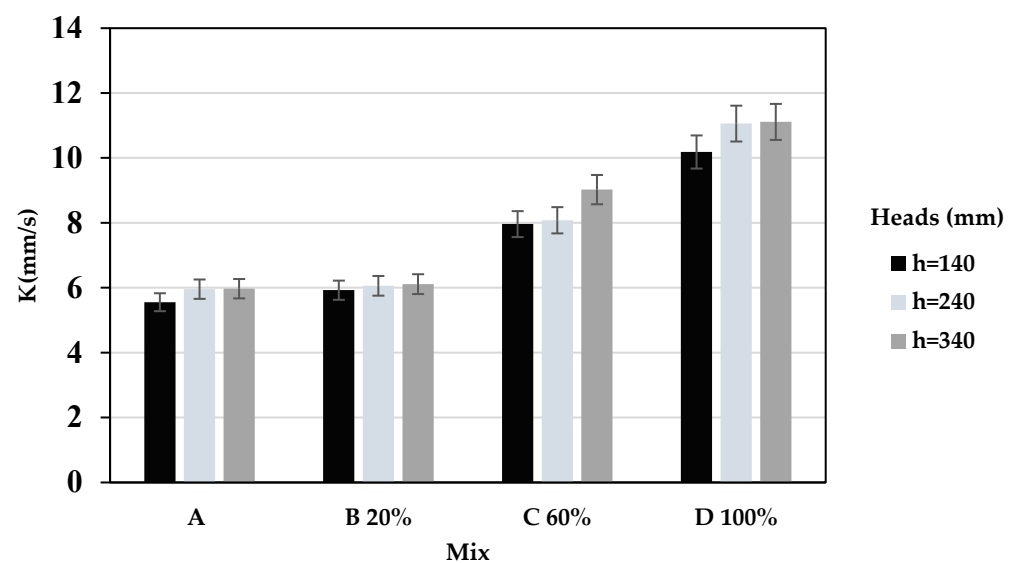


Figure 7. Permeability coefficient by constant head test.

Knowing that, pervious concrete is designed to have adequate porosity and a continuous matrix to facilitate the easy flow of water through it. According to the technical specification [72], the permeability of the pervious concrete should be at least  $5.4 \times 10^{-2}$  mm/s. The data presented in Figures 7 and 8, as well as the increase in porosity observed in Figure 9, indicate that this requirement is met in all of the studied mixtures. The incorporation of recycled aggregates into the mixtures, demonstrates the feasibility of using recycled aggregates in the production of pervious concrete.

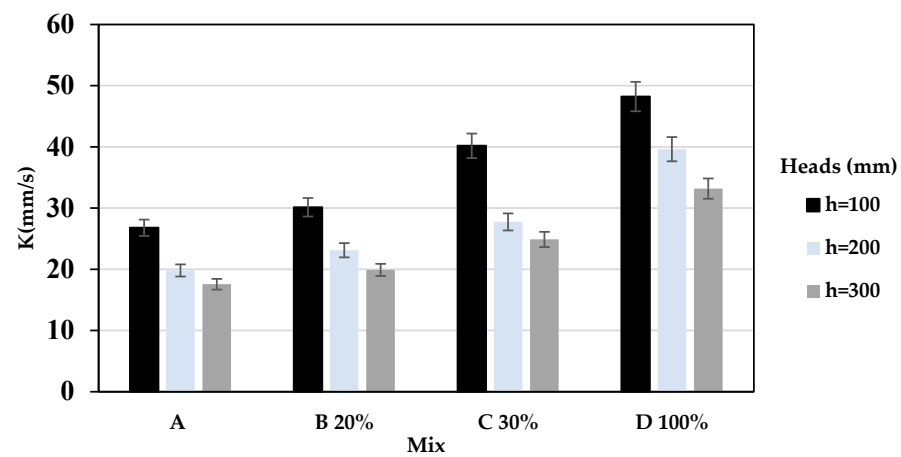
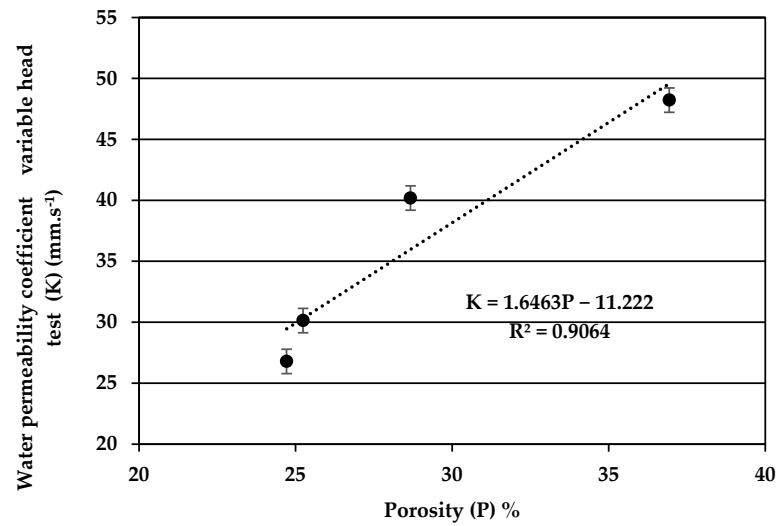
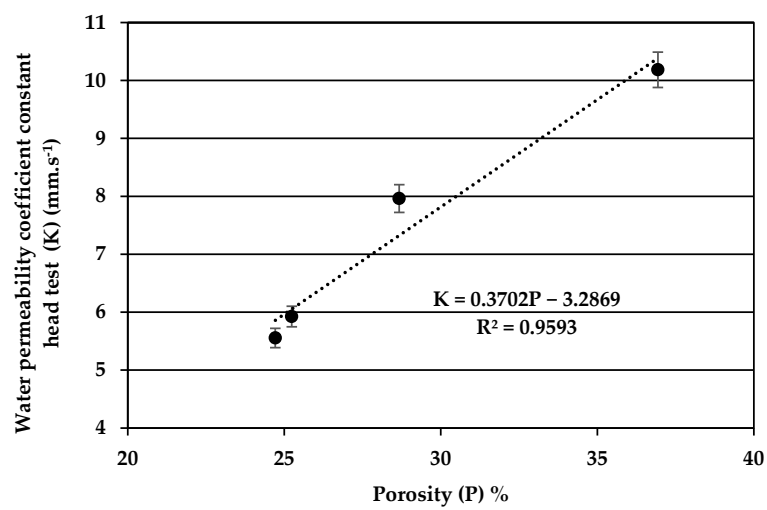


Figure 8. Permeability coefficient by falling head test.



(a)



(b)

Figure 9. Relationship between the porosity accessible to water  $P$  and the water permeability  $K$  obtained by the falling head test (a) and the constant head test (b).

Figure 8 illustrates the permeability at falling head loss. It has been found that the permeability coefficient decreases as the head increases from 100 mm to 300 mm in all the mixtures studied, regardless of the amount of RA added. This is probably due to a change in the flow pattern of the water from steady to turbulent flow as the piezometric head increases. When the piezometric head is large, a local circular current develops and significantly increases the resistance to flow, as previously demonstrated by studies [25,73]. The permeability coefficient varies from 17.6 mm/s in Mixture A to 48.2 mm/s in Mixture D. According to previous research [25,46], a porosity of 35% corresponds to a permeability coefficient of 35 mm/s [48] to 40 mm/s [21], which is in good agreement with the data obtained for Mixture D. Additionally, values obtained for the other mixtures are also effectively high, particularly given the rapid increase in permeability that has been observed for concretes with open porosity greater than 25% [23,39,74].

Figure 7 presents the permeability at a constant head loss, with values ranging from 5.56 to 11.11 mm/s. The permeability exhibits a positive correlation with the amount of recycled aggregate, as previously observed in other studies [37,52,62,75]. These findings are consistent with a typical range of permeability values from 2 to 12 mm/s. It is important to note that there is a difference in the results obtained from falling head and constant head tests, as reported in previous research [48].

#### 3.4. Water-Retaining and Absorption Coefficient under Wet Condition

The water capacity of the mixture designated as D100% underwent a decrease from 290 kg/m<sup>3</sup> to 211 kg/m<sup>3</sup> within 30 min of curing time. This decrease persisted and ultimately resulted in a final water capacity of 200 kg/m<sup>3</sup> at 1 h and 1 h and 30 min of curing time. The water capacity of the mixture designated as C60% was found to be lower than that of sample D100%, with a decrease from 200 kg/m<sup>3</sup> to 175 kg/m<sup>3</sup> observed within 30 min of curing time. This trend continued, with the water capacity ultimately reaching 128 kg/m<sup>3</sup> at 60 min and 156 kg/m<sup>3</sup> at 90 min of curing time. These observations are illustrated in Figure 10. In addition, Samples B20% and A were found to have an almost identical performance in terms of water capacity recording 150 kg/m<sup>3</sup>, 126 kg/m<sup>3</sup>, and 117 kg/m<sup>3</sup> at 30 min intervals between each measurement. Furthermore, the water capacity of all mixtures, including D100%, C60%, B20%, and Control A, were found to decrease to 180 kg/m<sup>3</sup>, 129 kg/m<sup>3</sup>, 87 kg/m<sup>3</sup>, and 86 kg/kg/m<sup>3</sup>, respectively, following a 24 h curing period.

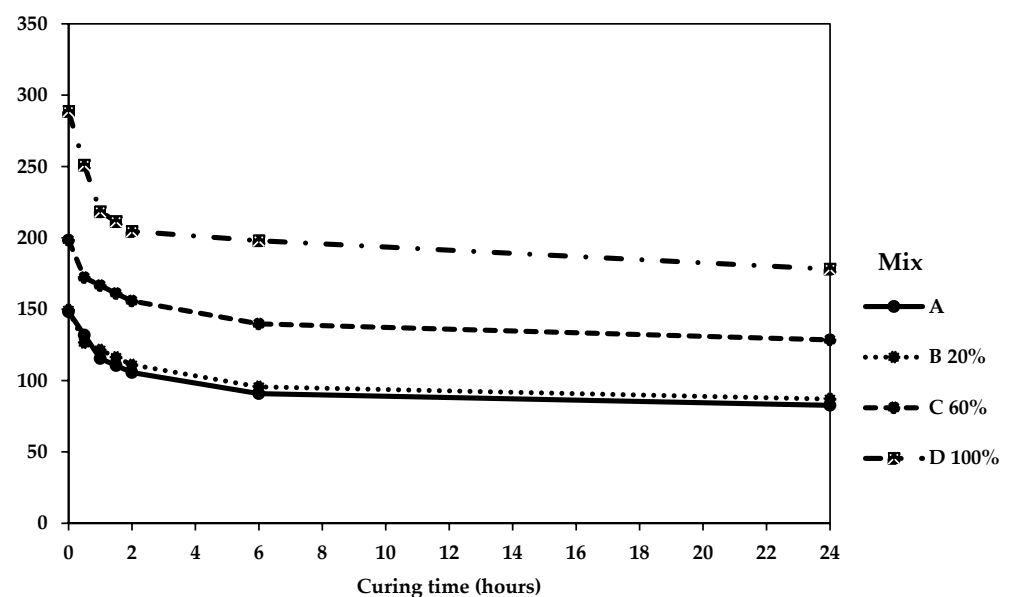
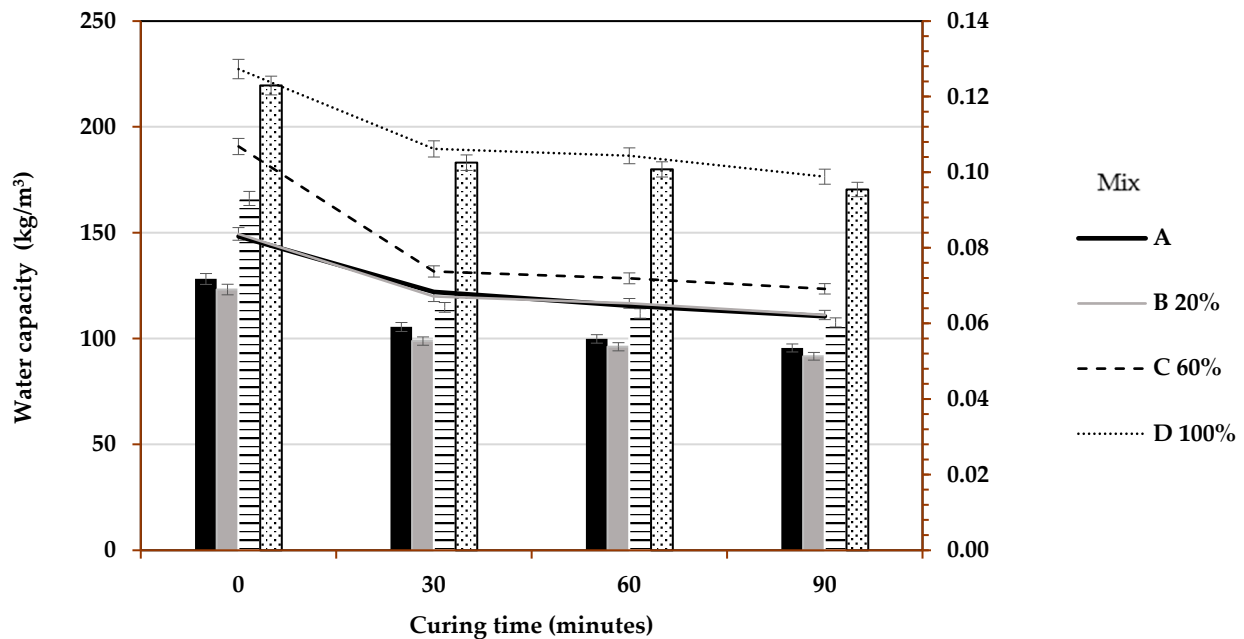


Figure 10. Relationship between curing time and water capacity.

The results of the absorption coefficient measurements, conducted over the first 90 min of the test and depicted in Figure 11, correlate with the results of the water retention capacity measurements. The absorption coefficient was observed to increase with an increase in the percentage of RA in the mixture, registering values of 7%, 9%, and 12% for Mixtures A and B20%, and Mixtures C60% and D100%, respectively, at the onset of the test. However, these values decreased to 5%, 6%, and 9% for Mixtures A and B20%, and C60% and D100%, respectively, after 90 min of testing.



**Figure 11.** Relationship between curing time, water capacity, and absorption coefficient.

Based on the obtained results, it can be inferred that the mixture designated as D100% exhibits significant and superior hydric performance when compared to Control A and other mixtures. This superiority is evident in its consistently high water retention capacity, which exceeds  $180 \text{ kg/m}^3$ . These observations align with the classification of D100% as a water-retaining block, as outlined in relevant sources [55,56].

Therefore, it can be inferred that the presence of RA as raw materials and their higher absorption coefficient (as seen in Table 2) serves to increase the water retention capacity of pavement. This enhancement not only improves the pavement's ability to mitigate urban heat islands, but also enhances the effectiveness of the watering solution (when adopted in wet conditions) aimed at artificially irrigating surfaces to cool the air and reduce surface temperature. The presence of pavement containing recycled aggregates allows for increased water storage capacity. As an example, the D100% mixture, once saturated with water, has the capability to retain  $200 \text{ kg/m}^3$  of water after 90 min of curing time, in comparison to the  $110 \text{ kg/m}^3$  retained by Control A. This increased water retention capacity results in a more efficient irrigation solution, as fewer watering cycles are required to achieve the desired surface temperature to mitigate urban heat island phenomena [8,9,13,17,70].

These findings are in correlation with several research studies that have investigated the potential of various materials as additives to pavements to improve their water-retaining capacity, reduce the urban heat island effect, and enhance thermal comfort. For example, one study [76] examined the use of water-holding fillers made of steel byproducts as additives to porous asphalt, which resulted in a reduction in the average surface temperature of 0.6 K compared to the infiltration of porous asphalt and a decrease in air temperature above the pavement of 0.5 K. The cooling effect of this water-holding pavement persisted for up to 3 days. Another study [77] investigated the use of fine blast-furnace powder as an additive to water-retentive asphalt, resulting in a surface temperature of up to 14 K lower



than the dense-graded asphalt pavement. Moreover, research studies that used bottom ash and peat moss as additives in pervious concrete, reported a surface temperature almost 18 K lower than asphalt after rainfall, and a maximum surface temperature difference of almost 9 K compared to a conventional porous pavement. Similarly, many studies [78] have explored the use of fly ash with a narrow particle size distribution in porous bricks, which reported lower surface temperatures of water-retentive materials and improvements in thermal comfort.

In conclusion, the results of this study provide evidence that the incorporation of recycled aggregates (RA) into a pavement mix can significantly improve the pavement's water retention capacity, which in turn can contribute to mitigating urban heat island phenomena under wet conditions. The D100% mixture, in particular, was found to exhibit superior water retention compared to the control mixture. Additionally, the incorporation of RA in the C60% mixture also exhibited positive results. These findings suggest that the use of RA in a pavement mix can play a valuable role in addressing the challenges associated with urban heat islands and promoting sustainable urban environments. It is also worth noting that this incorporation of RA does not compromise the perviousness of the pavement, as the high water-drainage capacity of the pervious concrete is conserved, which will categorize it as both a pervious and cool pavement simultaneously.

### 3.5. Water Absorption under Dry Condition

The results of the section height (Sh) measurements for Mixtures A, B, C, and D (Figure 12) provide insights into the height changes of the samples over time. These measurements are an indication of the physical behavior of the mixtures when exposed to water, and can provide insights into their potential performance in real-world applications, such as in pavement systems, to mitigate UHI.

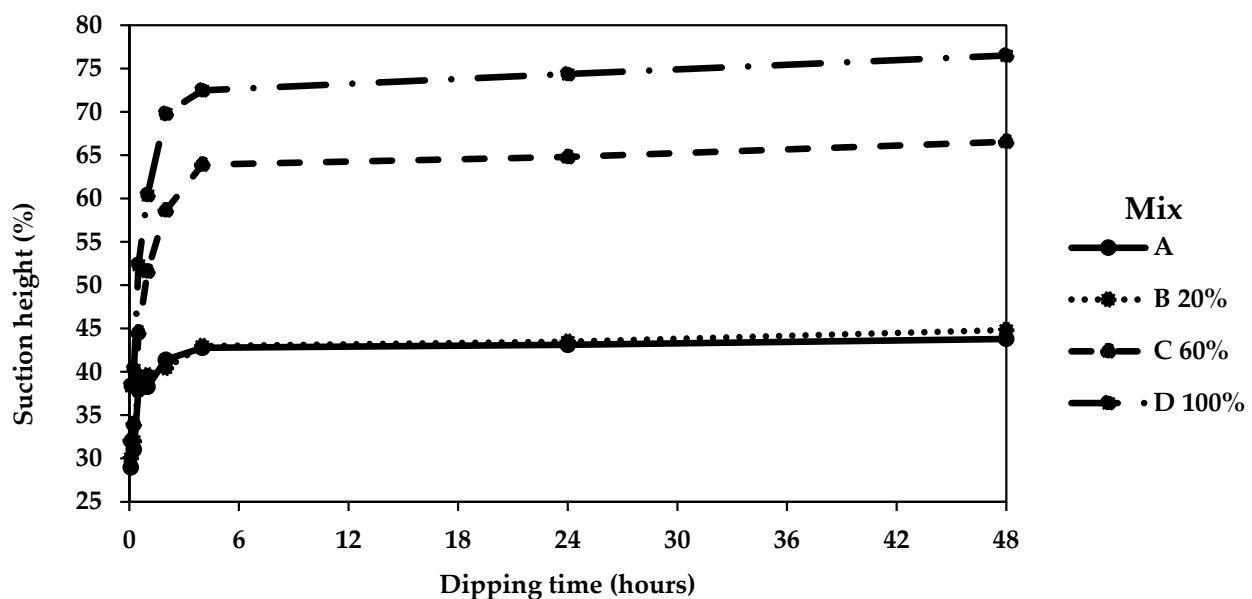


Figure 12. Relationship between dipping time and suction height.

Mixtures A, B, and C showed a relatively similar trend in their section height measurements, with an initial value of 33% after 5 min of immersion. This value then increased almost linearly to reach 40% for Mixtures A and B and 45% for Mixture C within 30 min. This indicates that these mixtures experienced an initial increase in height upon contact with water, which then leveled off to a stable value.

In contrast, Mixture D exhibited a more significant response to water immersion, with an initial section height of 38% in the first 5 min, which then increased to reach a value of 53% in 30 min. This suggests that this mixture experienced a greater initial expansion upon contact with water, which then slowed down.

The section height measurements for all the mixtures were also taken after 48 h, with 76% observed for Mixture D100%, 66% for C60% and 45% for Mixtures A and B20%.

In summary, the results of this study indicate that Mixtures C and D possess a notable hydric property, as outlined in relevant sources [55,56], in relation to their water retention capacity when compared to Control Mixture A. This superiority is attributed to the presence of recycled aggregates, which augment the water retention and absorption properties in a proportionate manner, as demonstrated in Figure 12.

These results indicate that after an extended period of water immersion, the height of all the mixtures had further increased, but with Mixture D100% showing the highest increase.

Furthermore, the results of the capillary absorption tests were found to be in concordance with the previously reported findings, as depicted in Figure 13. The capillary absorption tests revealed a capacity for upwelling water that reaches 33 kg of retained water per square meter in 48 h for Mixture D100%, 20 kg for Mixture C60%, 16 kg for Mixture B20%, and 12 kg for Control A.

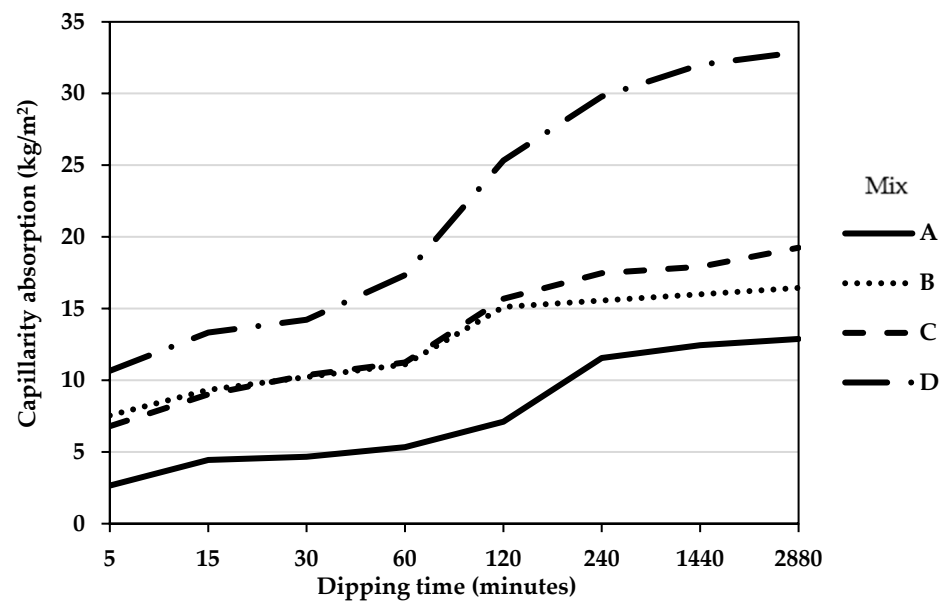


Figure 13. Capillarity absorption in function of dipping time for all mixtures.

In conclusion, the results of this study indicate that incorporating recycled aggregates (RA) into a pavement mix can significantly improve the pavement's water retention and absorption capacity. These findings are useful in assessing the potential performance of these mixtures in real-world applications, particularly in systems aimed at mitigating the challenges associated with urban heat islands. By increasing the pavement's ability to retain and absorb water, RA can contribute to reducing surface temperature and promoting more sustainable urban environments. This is especially important in areas where the water table is fed into the sub-layers or in cities where the sub-layers are artificially watered to cool surfaces and combat urban heat island phenomena [8,13,17,70].

The aforementioned findings are consistent with other research studies that have explored the use of industrial waste as a raw material for ceramic tiles, resulting in a practical solution for enhancing the water retention capacity of pavement tiles. The development of water-retentive ceramic tiles has yielded some of the most water-retentive tiles in the market, and the use of such tiles has resulted in a temperature reduction of almost 10 K, with the air above the tile being cooler by 1–2 K [79]. Additionally, the use of water-retentive materials with high capillary ability has been shown to be an effective solution for mitigating heat. The surface temperature of the proposed material was found to be 10 K cooler than the dry material and 25 K cooler than conventional asphalt [80].

Therefore, incorporating RA in pavement systems can be considered a promising strategy in addressing urban heat islands and promoting sustainable urban development.

This could be a promising strategy in addressing urban heat islands and promoting sustainable urban development by increasing the pavement's ability to retain and absorb water; RA can contribute to reducing surface temperature and promoting more sustainable urban environments.

### 3.6. Sorption/Desorption

The moisture sorption isotherms depicted in Figure 14 illustrate, for each mixture examined, the progression of moisture content in relation to the relative humidity of the surrounding air, at a fixed temperature of 23 °C.

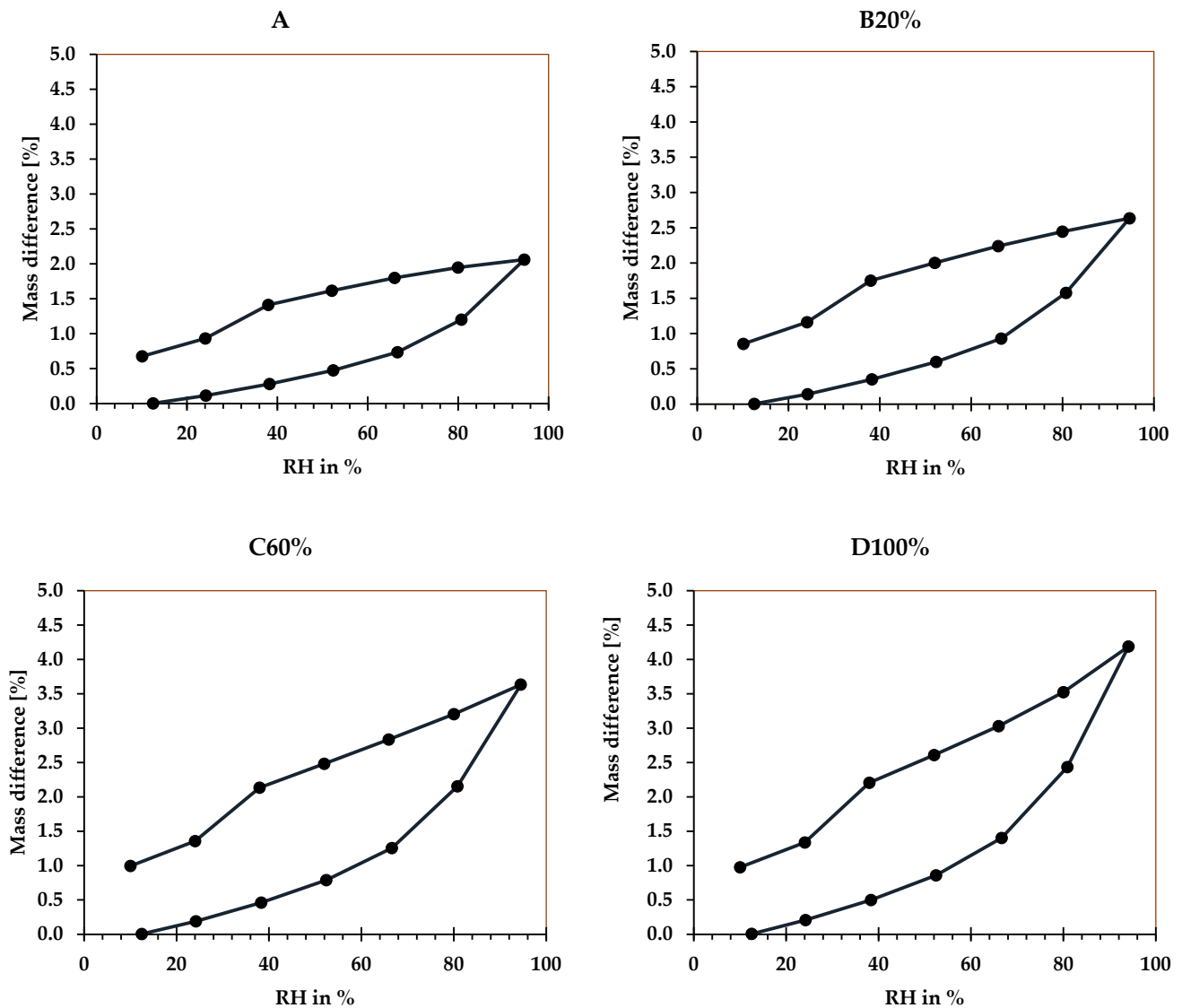


Figure 14. Sorption/desorption test for all mixtures.

It is evident that the increase in absorbed water vapor from the environment is proportional to the percentage of RA incorporated. This is evidenced by the observed 2%, 2.45%, 3.45%, and 4.25% variations in the mass for Mixtures A, B, C, and D, respectively, at a relative humidity of 95%. For a more comprehensive analysis of this sorption/desorption behavior, the raw materials (NA and RA) were characterized under the same conditions and parameters, as depicted in Figure 2. The results reveal that the sorption/desorption characteristics of the mixtures are directly correlated with the sorption/desorption characteristics of the raw materials. Specifically, at a relative humidity of 95%, recycled aggregates exhib-

ited a 2% mass variation compared to a 0.45% variation for natural aggregates, representing a 450% increase.

In Mixtures B, C, and D, the variation in mass was 26%, 76%, and 211% greater than that of Control Mixture A. These findings indicate that the inclusion of recycled aggregates results in a significant increase in the pavement's moisture absorption capacity.

In addition, it can be observed that the area between the sorption and desorption curves, also known as hysteresis, increases with the addition of recycled aggregates. This reduction in the mass difference between the different dosages is attributed to the inherent characteristics of the component, while the observed increase in hysteresis is likely the result of the porosity of the mixtures, as reported in sources [58,59]. This hypothesis is further supported by the data on the overall porosity of the mixtures as depicted in Figure 6, which indicates a noticeable increase in porosity with the incorporation of recycled aggregates. Thus, the findings on porosity can be correlated with those reported for the sorption/desorption curves. In particular, the higher porosity observed in the mixtures leads to an increase in the hysteresis zones depicted in Figure 14, thereby resulting in an overall increase in the hygroscopic nature of the mixtures.

The inclusion of such a pavement in a region with high relative humidity during the summer season will result in a significant absorption of moisture by the recycled pavement, and thereby contribute to the cooling of the surrounding air without the need for artificial means such as surface irrigation. As such, this cool recycled pervious concrete can represent a natural solution for mitigating urban heat island effects in regions with specific climatic conditions. These findings have been supported by studies in many sources [13,17,70,81].

#### 4. Conclusions

Experimental investigations on pervious concrete have demonstrated the practicality of utilizing recycled aggregates as a substitute for natural aggregates. This incorporation not only enhances the sustainability of the construction process by valorizing a waste material, but also improves the hydric and hygroscopic properties of the pervious pavement, thereby enhancing its functionality and ability to mitigate urban heat islands.

The primary outcomes of the current study are:

- The research conducted in this study determined that pervious concrete mixtures incorporating recycled aggregate (designated as B20% and C60%) possess mechanical properties comparable to those of pervious concrete mixtures utilizing natural aggregate (designated as A). However, mixtures consisting entirely of recycled aggregate (designated as D100%) exhibited a substantial decrease in mechanical strength, limiting their use for walkways and pedestrian trials;
- The findings of this study demonstrate that pervious concrete utilizing recycled aggregates displays substantial water permeability, owing to a high porosity that results in a large, interconnected pore system. Specifically, the water permeability for Mixtures D100% and C60% is approximately 50% and 80% higher, respectively, than that of Mixture A, as determined through both falling head and constant head permeability tests at various pressure heads. Additionally, Mixture B20% exhibited slightly higher values of permeability than Mixture A;
- The water capacity test results indicate the potential of incorporating recycled aggregates in pervious concrete to enhance hydric properties and mitigate urban heat island effects. The test results show that one cubic meter of Mixes D100% and C60% can absorb at least 80 and 45 L more water, respectively, compared to Mixes A and B20%. Mix D100% demonstrates the ability to maintain this difference for over an hour and a half, classifying it as a water-retaining block. This feature makes this type of pavement a viable solution in areas where artificial irrigation is utilized to combat urban heat island effects;
- The section height test results reveal that mixtures D100% and C60% reached 55% and 44%, respectively, after 30 min, in contrast to 40% for Mixtures B20% and A. These results indicate that increasing the proportion of recycled aggregates in pervious

concrete improves its hydric properties, which in turn enhances its effectiveness in combating urban heat island effects through the sub-watering method;

- The sorption/desorption test results emphasize the impact of recycled aggregates on the hydric and hygroscopic properties of pervious concrete. The test showed that the difference in mass in Mixtures B20%, C60%, and D100 was 26%, 76%, and 211% greater, respectively, than that in Control A. In addition, the area between the sorption and desorption curves, known as the hysteresis, was enhanced with the incorporation of recycled aggregate, resulting in an increase in the hygroscopicity of the mixtures. This enhancement in sorption and desorption capacity equips the recycled pavement with the capability to naturally mitigate the urban heat island in regions with hot and humid climates during warm seasons.

Regarding my perspectives for future work, I would like to conduct tests on a larger scale to evaluate the performance of the various mixes in terms of their thermal and durability properties.

In terms of testing on a larger scale, it would be beneficial to increase the sample size to ensure that the results obtained are statistically significant and representative. This could involve conducting experiments in multiple locations or replicating the experiments multiple times to reduce the impact of environmental variables.

When it comes to evaluating the thermal and durability properties of the different mixes, there are several methods that could be used. For thermal properties, techniques such as thermal conductivity measurements, specific heat capacity can be implemented. These techniques would help determine how the different mixes respond to changes in temperature and how they transfer heat.

For durability properties, tests such as freeze–thaw resistance and abrasion resistance can be used. These tests would help to evaluate how well the mixes withstand different types of stress and wear over time.

Overall, by conducting more extensive testing on a larger scale and evaluating the thermal and durability properties of the different mixes, we can gain a better understanding of their overall performance and identify areas for improvement.

**Author Contributions:** Writing—original draft preparation, B.H.; supervision, H.K., M.B., B.B. and N.S. All authors have read and agreed to the published version of the manuscript.

**Funding:** 69% co-funded project by INTERREG V FMA.

**Institutional Review Board Statement:** Not applicable.

**Informed Consent Statement:** Not applicable.

**Data Availability Statement:** Not applicable.

**Acknowledgments:** The results presented in this article were obtained in the framework of the collaborative project concrete solution dRaining for the Climate and environment (CIRCLE PROJECT), co-funded by the European Regional Development Fund through the European cross-border programme INTERREG V A France (Manche) Angleterre (FMA).

**Conflicts of Interest:** The authors declare no conflict of interest.

## References

1. Oke, T.R. The energetic basis of the urban heat island. *Q. J. R. Meteorol. Soc.* **1982**, *108*, 1–24. [[CrossRef](#)]
2. Oke, T. The urban energy balance. *Prog. Phys. Geogr. Earth Environ.* **1988**, *12*, 471–508. [[CrossRef](#)]
3. Arnfield, A.J. Two decades of urban climate research: A review of turbulence, exchanges of energy and water, and the urban heat island. *Int. J. Clim.* **2003**, *23*, 1–26. [[CrossRef](#)]
4. Al-Jabri, K.; Hago, A.W.; Al-Nuaimi, A.; Al-Saidy, A. Concrete blocks for thermal insulation in hot climate. *Cem. Concr. Res.* **2005**, *35*, 1472–1479. [[CrossRef](#)]
5. Grimmond, C.S.B.; Oke, T.R. Heat Storage in Urban Areas: Local-Scale Observations and Evaluation of a Simple Model. *J. Appl. Meteorol. Climatol.* **1999**, *38*, 922–940. [[CrossRef](#)]
6. Qin, Y.; Hiller, J.E. Understanding pavement-surface energy balance and its implications on cool pavement development. *Energy Build.* **2014**, *85*, 389–399. [[CrossRef](#)]

7. Akbari, H.; Rose, L.S. Characterizing the Fabric of the Urban Environment: A Case Study of Metropolitan Chicago, Illinois. October 2001. Available online: <https://buildings.lbl.gov/publications/characterizing-fabric-urban> (accessed on 15 January 2023).
8. Starke, P.; Göbel, P.; Coldewey, W.G. Urban evaporation rates for water-permeable pavements. *Water Sci. Technol.* **2010**, *62*, 1161–1169. [[CrossRef](#)]
9. Furumai, H.; Kim, J.; Imbe, M.; Okui, H. Recent application of rainwater storage and harvesting in Japan. Presented at the 3rd RWHM Workshop, Vienna, Austria, 11 September 2008.
10. Okada, K.; Matsui, S.; Isobe, T.; Kameshima, Y.; Nakajima, A. Water-retention properties of porous ceramics prepared from mixtures of allophane and vermiculite for materials to counteract heat island effects. *Ceram. Int.* **2008**, *34*, 345–350. [[CrossRef](#)]
11. Okada, K.; Ooyama, A.; Isobe, T.; Kameshima, Y.; Nakajima, A.; MacKenzie, K. Water retention properties of porous geopolymers for use in cooling applications. *J. Eur. Ceram. Soc.* **2009**, *29*, 1917–1923. [[CrossRef](#)]
12. Ishizuka, R.; Fujiwara, E.; Akagawa, H.; Ishizuka, R.; Fujiwara, E.; Akagawa, H. Study on applicability of water-feed-type wet block pavement to roadways. In Proceedings of the 8th International Conference on Concrete Block paving, San Francisco, CA, USA, 6–8 November 2006.
13. Santamouris, M. Using cool pavements as a mitigation strategy to fight urban heat island—A review of the actual developments. *Renew. Sustain. Energy Rev.* **2013**, *26*, 224–240. [[CrossRef](#)]
14. Li, H.; Harvey, J.T.; Holland, T.J.; Kayhanian, M. The use of reflective and permeable pavements as a potential practice for heat island mitigation and stormwater management. *Environ. Res. Lett.* **2013**, *8*, 15023. [[CrossRef](#)]
15. Pomerantz, M.; Akbari, H.; Chen, A.; Taha, H.; Rosenfeld, A. *Paving Materials for Heat Island Mitigation*; U.S. Department of Energy: Washington, DC, USA, 1997. [[CrossRef](#)]
16. Deo, O.; Neithalath, N. Compressive behavior of pervious concretes and a quantification of the influence of random pore structure features. *Mater. Sci. Eng. A* **2010**, *528*, 402–412. [[CrossRef](#)]
17. Qin, Y. A review on the development of cool pavements to mitigate urban heat island effect. *Renew. Sustain. Energy Rev.* **2015**, *52*, 445–459. [[CrossRef](#)]
18. Rehder, B.; Banh, K.; Neithalath, N. Fracture behavior of pervious concretes: The effects of pore structure and fibers. *Eng. Fract. Mech.* **2014**, *118*, 1–16. [[CrossRef](#)]
19. Shu, X.; Huang, B.; Wu, H.; Dong, Q.; Burdette, E.G. Performance comparison of laboratory and field produced pervious concrete mixtures. *Constr. Build. Mater.* **2011**, *25*, 3187–3192. [[CrossRef](#)]
20. Yang, J.; Jiang, G. Experimental study on properties of pervious concrete pavement materials. *Cem. Concr. Res.* **2003**, *33*, 381–386.
21. Carsana, M.; Tittarelli, F.; Bertolini, L. Use of no-fines concrete as a building material: Strength, durability properties and corrosion protection of embedded steel. *Cem. Concr. Res.* **2013**, *48*, 64–73. [[CrossRef](#)]
22. Shabalala, A.N.; Ekolu, S.O.; Diop, S.; Solomon, F. Pervious concrete reactive barrier for removal of heavy metals from acid mine drainage – column study. *J. Hazard. Mater.* **2017**, *323*, 641–653. [[CrossRef](#)]
23. *ACI 522R-10. Report on Pervious Concrete*; American Concrete Institute: Farmington Hills, MI, USA, 2010; 38p.
24. Neithalath, N. Development and Characterization of Acoustically Efficient Cementitious Materials. Ph.D. Thesis, Purdue University, West Lafayette, IN, USA, May 2004.
25. Zouaghi, A.; Nakazawa, T.; Imai, F.; Shinnishi, N. Permeability of No-Fines Concrete. *Trans. Jpn. Concr. Inst.* **1998**, *20*, 31–38.
26. National Union of Industry Careers and Building Materials. Available online: <https://www.unicem.fr/> (accessed on 12 December 2011).
27. Liu, J.; An, R.; Jiang, Z.; Jin, H.; Zhu, J.; Liu, W.; Huang, Z.; Xing, F.; Liu, J.; Fan, X.; et al. Effects of w/b ratio, fly ash, limestone calcined clay, seawater and sea-sand on workability, mechanical properties, drying shrinkage behavior and micro-structural characteristics of concrete. *Constr. Build. Mater.* **2022**, *321*, 126333. [[CrossRef](#)]
28. Thomas, C.; Setién, J.; Polanco, J.; Alaejos, P.; de Juan, M.S. Durability of recycled aggregate concrete. *Constr. Build. Mater.* **2013**, *40*, 1054–1065. [[CrossRef](#)]
29. Gesoğlu, M.; Güneyisi, E.; Mahmood, S.F.; Öz, H.; Öznur; Mermerdaş, K. Recycling ground granulated blast furnace slag as cold bonded artificial aggregate partially used in self-compacting concrete. *J. Hazard. Mater.* **2012**, *235–236*, 352. [[CrossRef](#)] [[PubMed](#)]
30. Yang, E.-I.; Kim, M.-Y.; Park, H.-G.; Yi, S.-T. Effect of partial replacement of sand with dry oyster shell on the long-term performance of concrete. *Constr. Build. Mater.* **2010**, *24*, 758–765. [[CrossRef](#)]
31. Sugiyama, M. The compressive strength of concrete containing tile chips, crushed scallop shells, or crushed roofing tiles, Gakuen Ronshu. *J. Hokkai-Gakuen Univ.* **2005**, *124*, 61–69.
32. Liu, J.; Li, Z.; Zhang, W.; Jin, H.; Xing, F.; Tang, L. The impact of cold-bonded artificial lightweight aggregates produced by municipal solid waste incineration bottom ash (MSWIBA) replace natural aggregates on the mechanical, microscopic and environmental properties, durability of sustainable concrete. *J. Clean. Prod.* **2022**, *337*, 130479. [[CrossRef](#)]
33. *NF EN 1097-6; Essais Pour Déterminer les Caractéristiques Mécaniques et Physiques des Granulats—Partie 6: Détermination de la Masse Volumique et du Coefficient D’Absorption D’Eau*. Association Française de Normalisation: Paris, France, February 2022.
34. *NF EN 933-1; Tests for Geometrical Properties of Aggregates—Part 1: Determination of Particle Size Distribution—Sieving Method*. Association Française de Normalisation: Paris, France, May 2012.
35. *NF EN 1097-1; Tests for Mechanical and Physical Properties of Aggregates—Part 1: Determination of the Resistance to Wear (Micro-Deval)*. Association Française de Normalisation: Paris, France, August 2011.



36. Grace, T.B.—Pervious Concrete Mix Proportioning Technical Bulletin | GCP Applied Technologies. Available online: <https://gcpat.com/en/solutions/products/adva-high-range-water-reducers/tb-0111-pervious-concrete-mix-proportioning> (accessed on 12 December 2008).
37. Tennis, P.D.; Leming, M.L.; Akers, D.J. *Pervious Concrete Pavements*; Portland Cement Association: Skokie, IL, USA, 2004.
38. Onstenk, E.; Aguado, A.; Eickschen, E.; Josa, A. Laboratory study of porous concrete for its use as top-layer of concrete pavements. In Proceedings of the Fifth International Conference on Concrete Pavement Design and Rehabilitation, West Lafayette, IN, USA, 20–22 April 1993.
39. Kevern, J. Advancements in Pervious Concrete Technology. Available online: <https://dr.lib.iastate.edu/entities/publication/b1e9ed4c-9851-4966-b554-da316534ef4c> (accessed on 3 January 2022).
40. Joung, Y.; Grasley, Z.C. *Evaluation and Optimization of Durable Pervious Concrete for Use in Urban Areas*; Southwest Region University Transportation Center: College Station, TX, USA, 2008.
41. Kevern, J.; Wang, K.; Suleiman, M.T.; Schaefer, V.R. Mix design development for pervious concrete in cold weather climates. In Proceedings of the 2005 Mid-Continent Transportation Research Symposium, Ames, IA, USA, 18–19 August 2005.
42. Farny, J.; In, F. Aging gracefully: Architectural concrete panels turn 40 years old. *Concr. Technol. Today* **2004**, *25*, 1–8.
43. Kevern, J.T.; Schaefer, V.R.; Wang, K. Evaluation of Pervious Concrete Workability Using Gyrotory Compaction. *J. Mater. Civ. Eng.* **2009**, *21*, 764–770. [[CrossRef](#)]
44. Chen, J.; Kwan, A.; Jiang, Y. Adding limestone fines as cement paste replacement to reduce water permeability and sorptivity of concrete. *Constr. Build. Mater.* **2014**, *56*, 87–93. [[CrossRef](#)]
45. Chia, K.S.; Zhang, M.-H. Water permeability and chloride penetrability of high-strength lightweight aggregate concrete. *Cem. Concr. Res.* **2002**, *32*, 639–645. [[CrossRef](#)]
46. Meiningner, R.C. No-fines pervious concrete for paving. *Concr. Int.* **1988**, *10*, 20–27.
47. Mulligan, A.M. Attainable Compressive Strength of Pervious Concrete Paving Systems. Master’s Thesis, University of Central Florida, Orlando, FL, USA, 2005.
48. Nguyen, D.H.; Boutouil, M.; Sebaibi, N.; Leleyter, L.; Baraud, F. Valorization of seashell by-products in pervious concrete pavers. *Constr. Build. Mater.* **2013**, *49*, 151–160. [[CrossRef](#)]
49. *NF EN 12390*; Testing Hardened Concrete—Part 3: Compressive Strength of Test Specimens. Association Française de Normalisation: Paris, France, 2003.
50. *NF EN 1338*; Concrete Paving Blocks—Requirements and Test Methods. Association Française de Normalisation: Paris, France, 2010.
51. Mata, L.A. Sedimentation of Pervious Concrete Pavement Systems. Ph.D. Thesis, North Carolina State University, Raleigh, NC, USA, 2008.
52. Montes, F.; Haselbach, L. Measuring Hydraulic Conductivity in Pervious Concrete. *Environ. Eng. Sci.* **2006**, *23*, 960–969. [[CrossRef](#)]
53. *NF ISO 5017*; Produits Réfractaires Façonnés Denses—Détermination de la Masse Volumique Apparente, de la Porosité Ouverte et de la Porosité Totale. Association Française de Normalisation: Paris, France, 2013.
54. Das, B.M. *Principles of Geotechnical Engineering*; Cengage Learning: Boston, MA, USA, 2021.
55. Karasawa, A.; Toriiminami, K.; Ezumi, N.; Kamaya, K. Evaluation of performance of water-retentive concrete block pavements. In Proceedings of the 8th International Conference on Concrete Block Paving, San Francisco, CA, USA, 6–8 November 2006.
56. Yamamoto, T.; Maki, T.; Honda, T. Discussions on assessment and quality standards of water-retaining concrete block. In Proceedings of the 8th International Conference on Concrete Block Paving, San Francisco, CA, USA, 6–8 November 2006.
57. *NF EN ISO 12571*; Hygrothermal Performance of Building Materials and Products—Determination of Hygroscopic Sorption Properties. Association Française de Normalisation: Paris, France, 2013.
58. Alassaad, F.; Touati, K.; Levacher, D.; Sebaibi, N. Impact of phase change materials on lightened earth hygroscopic, thermal and mechanical properties. *J. Build. Eng.* **2021**, *41*, 102417. [[CrossRef](#)]
59. Bouasria, M.; El Mendili, Y.; Benzaama, M.-H.; Pralong, V.; Bardeau, J.-F.; Hennequart, F. Valorisation of stranded *Laminaria digitata* seaweed as an insulating earth material. *Constr. Build. Mater.* **2021**, *308*, 125068. [[CrossRef](#)]
60. Rizvi, R.; Tighe, S.L.; Norris, J.; Henderson, V. Incorporating recycled concrete aggregate in pervious concrete pavements. In Proceedings of the 2009 Annual Conference and Exhibition of the Transportation Association of Canada: Transportation in a Climate, Vancouver, BC, Canada, 18–21 October 2009.
61. Ghafoori, N.; Dutta, S. Laboratory Investigation of Compacted No-Fines Concrete for Paving Materials. *J. Mater. Civ. Eng.* **1995**, *7*, 183–191. [[CrossRef](#)]
62. Sebaibi, N. Valorisation des composites thermodurcissables issus du recyclage dans une matrice cimentaire: Application aux bétons à ultra-haute performance. These de doctorat, Artois. 2010. Available online: <https://www.theses.fr/2011ARTO0201> (accessed on 15 March 2023).
63. Poon, C.S.; Chan, D. Paving blocks made with recycled concrete aggregate and crushed clay brick. *Constr. Build. Mater.* **2006**, *20*, 569–577. [[CrossRef](#)]
64. Bravo, M.; de Brito, J.; Pontes, J.; Evangelista, L. Mechanical performance of concrete made with aggregates from construction and demolition waste recycling plants. *J. Clean. Prod.* **2015**, *99*, 59–74. [[CrossRef](#)]
65. Yap, S.P.; Chen, P.Z.C.; Goh, Y.; Ibrahim, H.A.; Mo, K.H.; Yuen, C.W. Characterization of pervious concrete with blended natural aggregate and recycled concrete aggregates. *J. Clean. Prod.* **2018**, *181*, 155–165. [[CrossRef](#)]



66. Ibrahim, H.A.; Razak, H.A. Effect of palm oil clinker incorporation on properties of pervious concrete. *Constr. Build. Mater.* **2016**, *115*, 70–77. [[CrossRef](#)]
67. Crouch, L.K.; Pitt, J.; Hewitt, R. Aggregate Effects on Pervious Portland Cement Concrete Static Modulus of Elasticity. *J. Mater. Civ. Eng.* **2007**, *19*, 561–568. [[CrossRef](#)]
68. Kevern, J.T.; Haselbach, L.; Schaefer, V.R. Hot Weather Comparative Heat Balances in Pervious Concrete and Impervious Concrete Pavement Systems. *J. Heat Isl. Inst. Int.* **2012**, *7*, 2012.
69. Kevern, J.T.; Schaefer, V.R.; Wang, K. Temperature Behavior of Pervious Concrete Systems. *Transp. Res. Rec. J. Transp. Res. Board* **2009**, *2098*, 94–101. [[CrossRef](#)]
70. Vujovic, S.; Haddad, B.; Karaky, H.; Sebaibi, N.; Boutouil, M. Urban Heat Island: Causes, Consequences, and Mitigation Measures with Emphasis on Reflective and Permeable Pavements. *CivilEng* **2021**, *2*, 459–484. [[CrossRef](#)]
71. Bamforth, P.B. The water permeability of concrete and its relationship with strength. *Mag. Concr. Res.* **1991**, *43*, 233–241. [[CrossRef](#)]
72. PTV122. *Technical Specifications for Permeable Concrete Paving Blocks and Slabs*, 2nd ed.; PROBETON: Brussel, Belgium, 2005.
73. Aoki, Y. Development of Pervious Concrete. Master's Thesis, University of Technology Sydney, Sydney, Australia, 2009.
74. Nguyen, D.H.; Sebaibi, N.; Boutouil, M.; Leleyter, L.; Baraud, F. A modified method for the design of pervious concrete mix. *Constr. Build. Mater.* **2014**, *73*, 271–282. [[CrossRef](#)]
75. Wang, K.; Schaefer, V.R.; Kevern, J.T.; Suleiman, M.T. Development of mix proportion for functional and durable pervious concrete. In Proceedings of the NRMCA Concrete Technology Forum: Focus on Pervious Concrete, Nashville, TN, USA, 24–25 May 2006; pp. 1–12.
76. Nakayama, T.; Fujita, T. Cooling effect of water-holding pavements made of new materials on water and heat budgets in urban areas. *Landsc. Urban. Plan.* **2010**, *96*, 57–67. [[CrossRef](#)]
77. Takahashi, K.; Yabuta, K. Road Temperature Mitigation Effect of “Road Cool” a Water-Retentive Material Using Blast Furnace Slag. *JFE. Tech. Rep.* **2009**, *19*, 58–62.
78. Akagawa, H.; Takebayashi, H.; Moriyama, M. Experimental study on improvement of human thermal environment on a watered pavement and a highly reflective pavement. *J. Environ. Eng. (Trans. AIJ)* **2008**, *73*, 85–91. [[CrossRef](#)]
79. Ozaki, T.; Suzuki, Y. Study on the contribution of water-retentive ceramic tile to the reduction of environment heat accumulation. *Proc. Hydraul. Eng.* **1998**, *42*, 61–66. [[CrossRef](#)]
80. Akagawa, H.; Komiya, H. Experimental study on pavement system with continuous wet surface. *J. Arch. Plan. (Trans. AIJ)* **2000**, *65*, 79–85. [[CrossRef](#)]
81. Alssaad, F.; Touati, K.; Levacher, D.; El Mendili, Y.; Sebaibi, N. Improvement of cob thermal inertia by latent heat storage and its implication on energy consumption. *Constr. Build. Mater.* **2022**, *329*, 127163. [[CrossRef](#)]

**Disclaimer/Publisher's Note:** The statements, opinions and data contained in all publications are solely those of the individual author(s) and contributor(s) and not of MDPI and/or the editor(s). MDPI and/or the editor(s) disclaim responsibility for any injury to people or property resulting from any ideas, methods, instructions or products referred to in the content.